The Prospects for Quantum Information Processing Using Electron Spin in Semiconductors

A Semiconductor Based Teleportation Repeater for Long Distance Quantum Communications:

Eli Yablonovitch, UCLA Electrical Engineering Dept.
Prof. Karoly Holczer, UCLA Physics Dept.
Prof. HongWen Jiang, UCLA Physics Dept.
Dr. Hideo Kosaka, Visiting Scientist, UCLA & NEC Japan
Mr. Thomas Szkopek, student, UCLA EE Dept.
Mr. Deepak Rao, student, UCLA EE Dept.
Dr. Hans Robinson, post-doc, UCLA EE Dept.
Dr. Rutger Vrijen, former post-doc, now at SUN Microsystems Lab

1 qu-bit≡1 spin

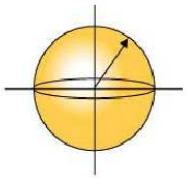

1 spin: $|\Psi\rangle = c_1|0\rangle + c_2|1\rangle$

2 spins $|\Psi\rangle = c_1|00\rangle + c_2|01\rangle + c_3|10\rangle + c_4|11\rangle$

3 spins $|\Psi\rangle = c_1|000\rangle + c_2|001\rangle + c_3|010\rangle + c_4|011\rangle + c_5|100\rangle + c_6|101\rangle + c_7|110\rangle + c_8|111\rangle$

•
•
•

1 spin → 2 complex numbers
2 spins → 4 complex numbers
3 spins → 8 complex numbers

N spins → 2^N complex numbers

No. of digital classical configurations = 2^N

No. of unentangled quantum configurations = $(2^\alpha)^N$

($\alpha \equiv$ bits of analog precision)

No. of entangled quantum configurations = $\left(2^\alpha\right)^{2^N}$

2^{2^N} scaling:

How many classical bits do we need to specify a wave function with 2 bit accuracy?

Consider N=34 atoms
$2^{34} \times 2^2 = 2^{36} = 80$ Gbits =10Gbytes
"1 hard disk"

Consider N=61 atoms
$2^{61} \times 2^2 = 2^{63} = 8\times10^{18}$ bits $=10^8$ hard disks
"world-wide annual production"

Consider N=94 atoms
$2^{94} \times 2^2 = 2^{96} = 8\times10^{28}$ bits $=10^{18}$ hard disks
"world-wide continuous production for the age of the universe"

ordinary bit: $\alpha|0\rangle + \beta|1\rangle$

Now allow for conditional probability (also called entanglement)

$$\alpha|0\rangle + \beta|1\rangle$$
$$\uparrow \quad \uparrow$$

α, β depend on what all the other (N-1) spins are doing
$\Rightarrow 2^{N-1}$ conditional probabilities and Huge Complexity

- You do not have internal access to quantum complexity.
- The entanglement collapses when you measure.
- There are N output bits and only 2^N possible answers.

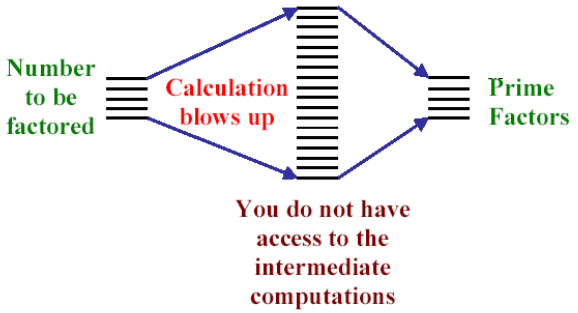

Algorithms:

Shor's factorization algorithm (1994)

Kitaev's factorization algorithm (1996)

Near term:

Small computer for error correction of Quantum Cryptography-

"Quantum Repeater"

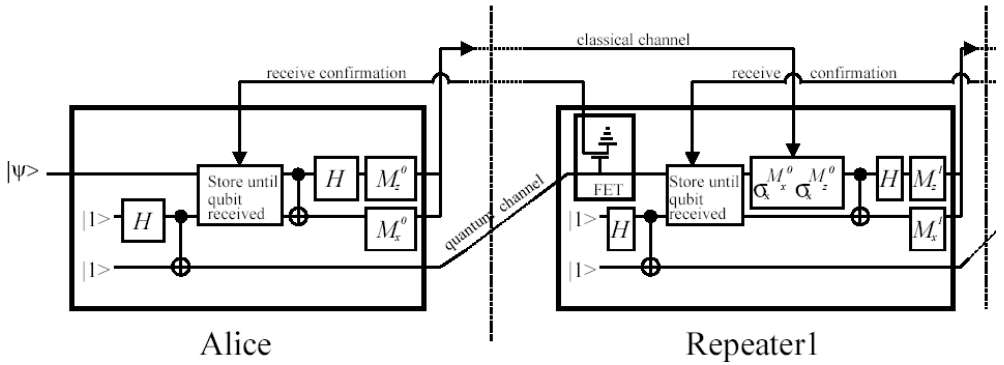

Error Correction:

Use redundancy, substitute 3 spins for one:

$|1\rangle \Rightarrow |1\rangle|1\rangle|1\rangle$ Robust against

$|0\rangle \Rightarrow |0\rangle|0\rangle|0\rangle$ spin-flips

Phase Error Correcting Code:

$|a\rangle \Rightarrow (|0\rangle + |1\rangle)(|0\rangle + |1\rangle)(|0\rangle + |1\rangle)$

$|b\rangle \Rightarrow (|0\rangle - |1\rangle)(|0\rangle - |1\rangle)(|0\rangle - |1\rangle)$

$|a\rangle \Rightarrow |000\rangle+|001\rangle+|010\rangle+|011\rangle+|100\rangle+|101\rangle+|110\rangle+|111\rangle$

$|b\rangle \Rightarrow |000\rangle-|001\rangle-|010\rangle+|011\rangle-|100\rangle+|101\rangle+|110\rangle-|111\rangle$

More compact phase error correcting code:

$|a\rangle \Rightarrow |000\rangle+|011\rangle+|101\rangle+|110\rangle$

$|b\rangle \Rightarrow |001\rangle+|010\rangle+|100\rangle+|111\rangle$

Shor's original phase and amplitude error correcting code:

$|a\rangle \Rightarrow (|000\rangle + |111\rangle)(|000\rangle + |111\rangle)(|000\rangle + |111\rangle)$

$|b\rangle \Rightarrow (|000\rangle - |111\rangle)(|000\rangle - |111\rangle)(|000\rangle - |111\rangle)$

requires 9 qubits.

Threshold:

Error Rate must be $<10^{-3}$ or 10^{-4}

Classical Error Correction:

N bits plotted in N-dimensional space:

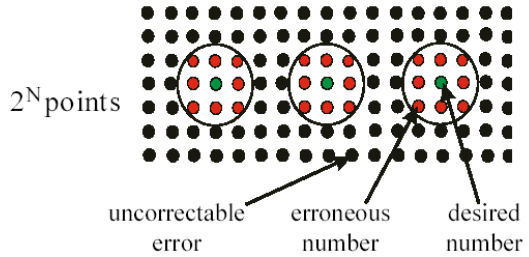

Because N-dimensional space is huge,
the overhead on un-used points is relatively minor.

(N-k) dimensions of useful numbers.
k dimensions of redundancy.

- Floppy disks
- CD-ROMs
- Digital Communication
- Voice Communication

Simplest case of 3-dim space,
$2^3 = 8$ points

Code	Errors
$\|000\rangle$	$\|100\rangle$, $\|010\rangle$, $\|001\rangle$
$\|111\rangle$	$\|011\rangle$, $\|101\rangle$, $\|110\rangle$

Quantum Error Correction:

(N-k) dimensional Hilbert space

2^{N-k} points

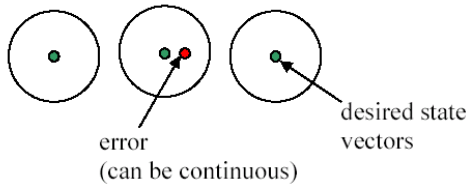

Unitary rotation of error into the k redundant dimensions.

Errors build up in the redundant degrees of freedom,
and must be purged from time to time.

Quantum Error Correction works, only if errors are $<10^{-4}$

•Physical realizations of qubits:

- •photon polarization
- •electron spin
- •nuclear spin
- •electron states in a trapped ion/atom
- •Anharmonic LC oscillator states in a Josephson junction ring

Spins are favorable because of:

- Less environmental disturbance
- Less spontaneous emission and quantum noise at RF frequencies.
- •electron spin transitions respond faster and easier to detect than nuclear spins
- •But, superconducting rings are limited mainly by dissipation, that can be low

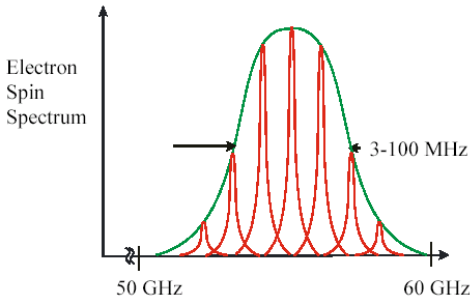

Electron spin in Si at ~ 1°K:
$T_1 \geq 1$ hour
10 nsec $\leq T^*_2 \leq$ 500nsec
$T_2 \geq 0.5$msec

Nuclear Spin $T_1 > 1$ hour.
Nuclear Spin T_2 is not measured.

Spin-Echo measurements:

J.P. Gordon et al, Physical Review Letters 1, 368 (1958)

M. Chiba & A. Hirai, J. Phy. Society of Japan 33, 730 (1972)

Electron Spin
Line Broadening Mechanisms:

1. Spin-orbit coupling
vibrations change the g-factor;
proportional to T^4

2. Dyakonov $\vec{v}\times\vec{E}_{eff}$ mechanism (in III-V's)

3. Hyperfine coupling to nuclei:

$$\sum_n \vec{\mu}_e \cdot \vec{\mu}_n \frac{8\pi}{3}\left|\Psi(r_n)\right|^2 + \frac{3(\vec{\mu}_e\cdot\hat{r})(\vec{\mu}_n\cdot\hat{r}) - \vec{\mu}_e\cdot\vec{\mu}_n}{r^3}$$

isotopically pure ^{28}Si or Ge: 99.92% ^{28}Si is available.

4. Electrical Noise on the gates

5. Electron Spin-Electron Spin interaction;
Figure-of-Merit = On/Off ratio of Exchange Interaction

In the chart of nuclides there are no spin zero nuclei in column III or column V of the periodic table!

III	IV	V
5 B^{11}	6 C^{12} 99% spinless	7 N^{14}
13 Al^{27}	14 Si^{28} 95% spinless	15 P^{31}
31 Ga^{69}	32 Ge^{74} 92% spinless	33 As^{27}
49 In^{115}	50 Sn^{120}	51 Sb^{121}

What do we really know about T_2 & T_2^* ?

Electron Spins in **Silicon** at low temps		
	Homogeneous dephasing time T_2	Inhomogeneous dephasing time T_2^*
Trapped electrons	0.3msec-0.5msec Spin Echo in n-Si	100nsec-1μsec ESR in n-Si
Mobile electrons	100nsec-10μsec magneto-resistive ESR in 2d Si-Ge electron-gas	No Inhomogeneous Broadening

Electron Spins in **III-V's** at low temps		
	Homogeneous dephasing time T_2	Inhomogeneous dephasing time T_2^*
Trapped electrons	Not Known! Spin Echo in very lightly doped n-GaAs, to avoid exchange interactions	≈3nsec ESR in n-GaAs
Mobile Electrons	0.1nsec-500nsec (a) Awschalom et al, optical ESR (b) magneto-resistive ESR in 2-d e-gas	No Inhomogeneous Broadening

Table 1. A short list of "long" T_2 values in comparison with the value found in n-type Si:

Material	temperature	T_2
γ-irradiated quartz	300K	2-5 μsec
N-V centers in diamond, (*price/purity dependent*)	300K	2-100 μsec
N@C60 (spin 3/2) [1]	300K solution	120 μsec
Phosphorus in Si	<12°K	250 μsec

Benefits of a Carbon Host for electron spin:

- Low Z ⇒ small spin-orbit dephasing.
- High Debye temperature ⇒ less phonon dephasing.
- 99% spin free C^{12}, only 1% C^{13}, less hyperfine broadening.
- Larger binding energies and energy spacings

300°K quantum information processor?

[1]Knapp et al, Chem. Phys. Lett. 272, p.433 (1997)

Electron Spin Dephasing by Nuclear Spin Diffusion

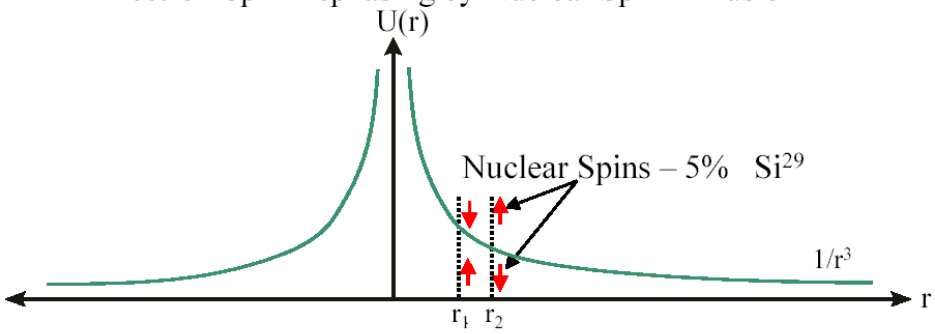

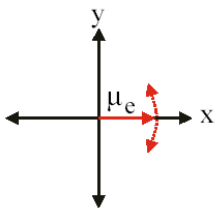

$$\Delta\omega = \sum_n \frac{1}{\hbar r^3}\left[3(\mu_n\cdot\hat{r})(\mu_e\cdot\hat{r}) - (\mu_n\cdot\mu_e)\right]$$

$$e^{i\int_0^t \Delta\omega(t')dt'} = e^{i\int_0^t A\sqrt{t'}dt'} = e^{i\frac{2}{3}At^{3/2}} \Longrightarrow \exp\left\{-(t/t_0)^3\right\}$$

Spin Dephasing Lifetime $t_0 \sim \left[\frac{1}{N_{Si^{29}}}\right]^{\alpha}$ ← model dependent exponent

Isotopic impurity density

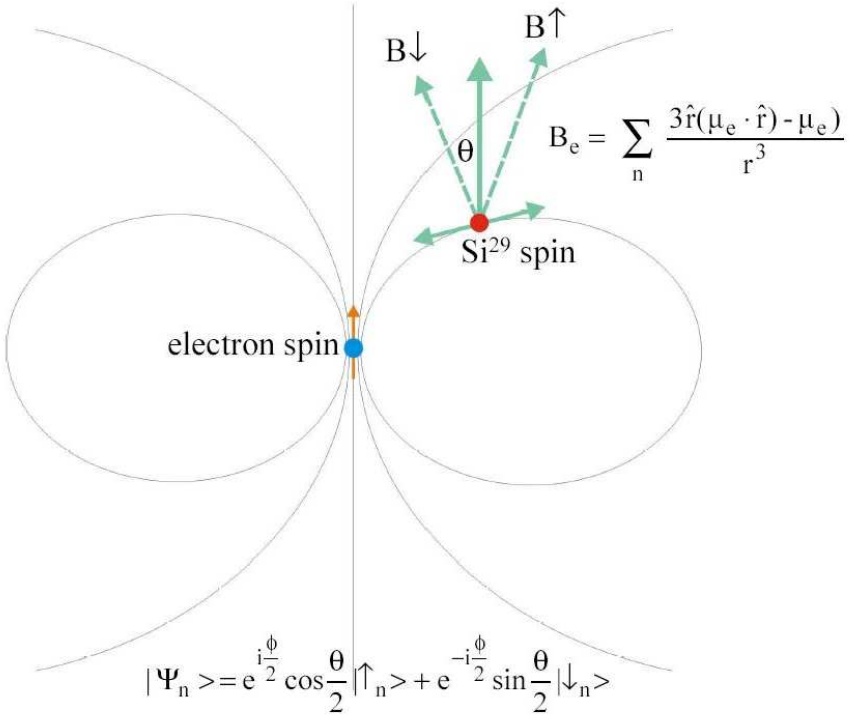
B↓
B↑
θ
$B_e = \sum_n \frac{3\hat{r}(\mu_e \cdot \hat{r}) - \mu_e}{r^3}$
Si29 spin
electron spin
$|\Psi_n> = e^{i\frac{\phi}{2}} \cos\frac{\theta}{2}|\uparrow_n> + e^{-i\frac{\phi}{2}} \sin\frac{\theta}{2}|\downarrow_n>$

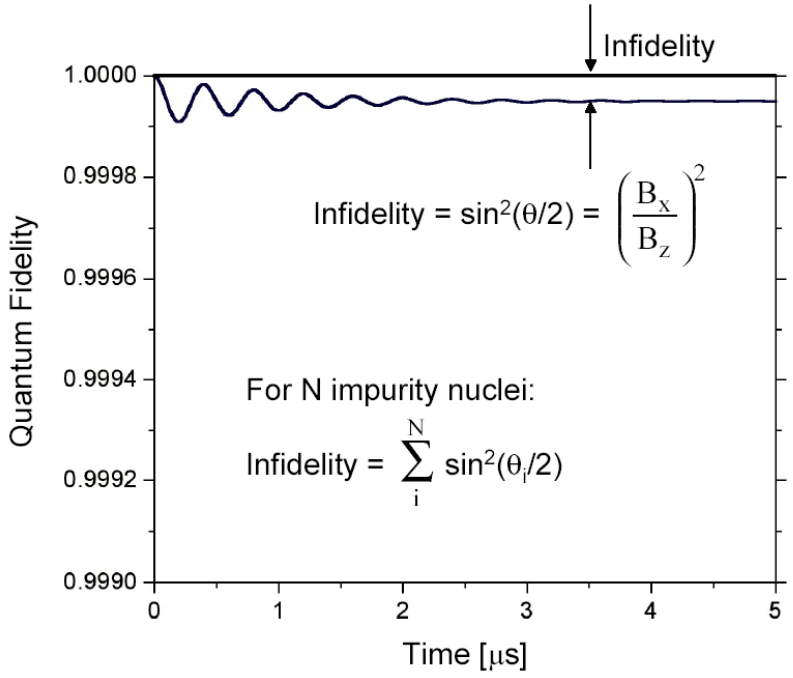
Infidelity
1.0000
0.9998
0.9996
0.9994
0.9992
0.9990
Quantum Fidelity
Infidelity = $\sin^2(\theta/2) = \left(\frac{B_x}{B_z}\right)^2$
For N impurity nuclei:
Infidelity = $\sum_i^N \sin^2(\theta_i/2)$
0
1
2
3
4
5
Time [μs]

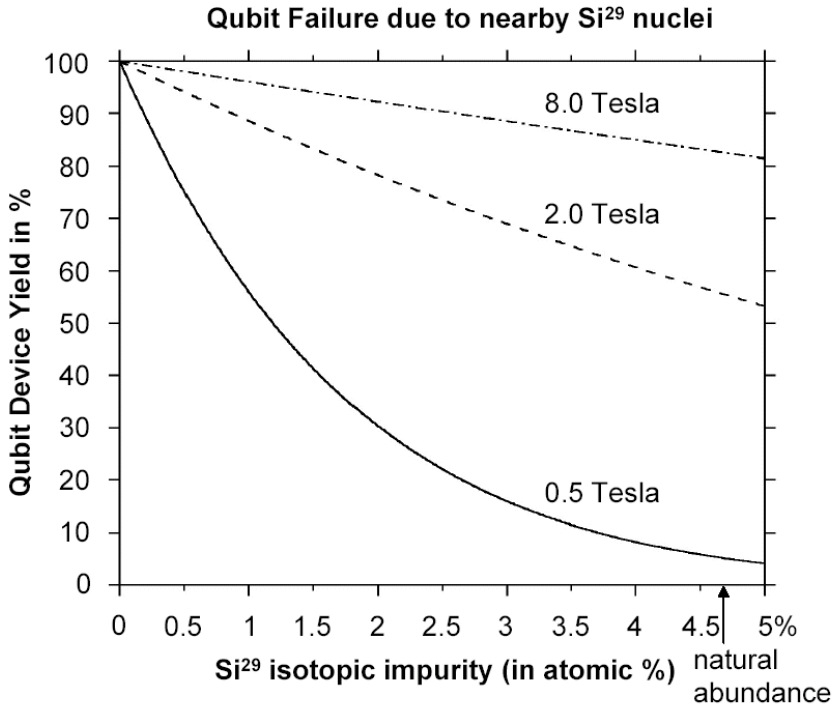
Qubit Failure due to nearby Si29 nuclei
Qubit Device Yield in %
100
90
80
70
60
50
40
30
20
10
0
8.0 Tesla
2.0 Tesla
0.5 Tesla
0
0.5
1
1.5
2
2.5
3
3.5
4
4.5
5%
Si29 isotopic impurity (in atomic %)
natural abundance

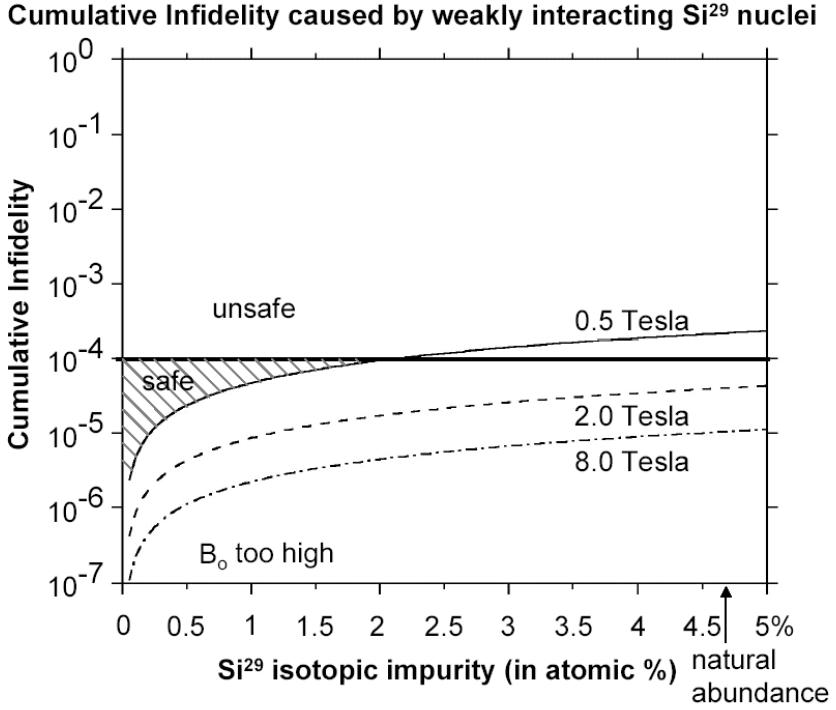
Cumulative Infidelity caused by weakly interacting Si29 nuclei
Cumulative Infidelity
10^0
10^{-1}
10^{-2}
10^{-3}
10^{-4}
10^{-5}
10^{-6}
10^{-7}
unsafe
0.5 Tesla
safe
2.0 Tesla
8.0 Tesla
B_o too high
0
0.5
1
1.5
2
2.5
3
3.5
4
4.5
5%
Si29 isotopic impurity (in atomic %)
natural abundance

Nuclear Spins can also produce an initial step Projection Error in many types of macro-scopic qubits!

A macroscopic qubit can cause un-intentional off-resonant NMR, whenever electric currents exist.

For example, a flux quantum is associated with B ~ 1 milli-gauss
This can produce an NMR frequency of f ~ 6Hz
At a clock period of 100nsec,
this can disturb the nuclear spins by ~10^{-7}radians

This would produce an infidelity of ~10^{-14}

But if there are ~10^{10} nuclear spins in the sample,

The total infidelity would be ~10^{-4}, enough to be concerned.

Conduction bands in Si & Ge

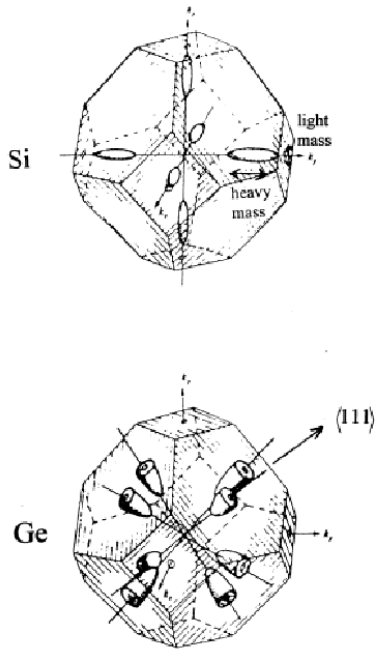

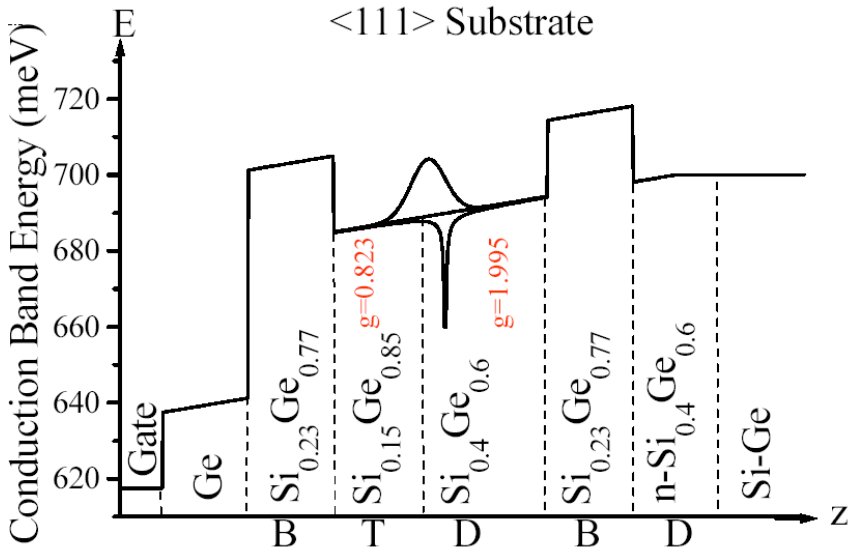

Band Structure Engineering is famous for controlling effective mass.

Thus it controls g-factor also:

$$g\text{-}2 \sim -\frac{\text{spin}-\text{orbit coupling}}{E_g}\left(\frac{m}{m_{eff}}-1\right)$$

"g-factor engineering"

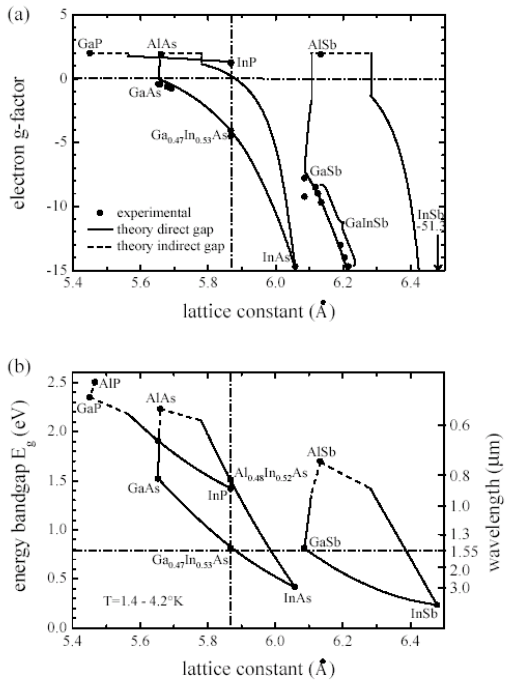

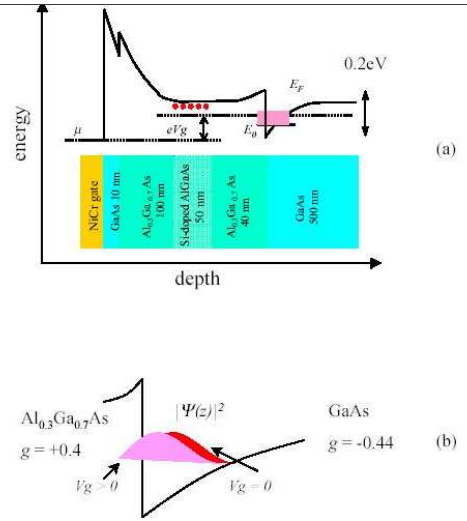

Figure 1. (a) Schematic diagram of the conduction band of the modulation doped GaAs/$Al_{0.3}$ $Ga_{0.7}$As heterostructure. Fermi level, E_F, the chemical potential, μ, and the lowest energy level of the quantum well, E_0, are indicated. (b) The two-dimensional electrons are trapped in the "triangle" shaped quantum well near the interface of the GaAs and $Al_{0.3}$ $Ga_{0.7}$As materials. The electron wavefunction shifts back and forth for bias voltage V_g=zero and a positive bias voltage.

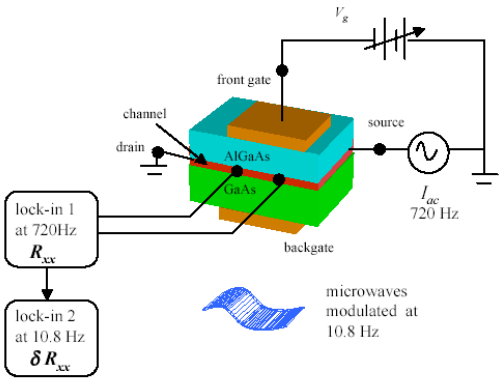

Figure 2. Diagram of the experimental setup for monitoring electron spin resonance and for controlling the spin orientation.

Spin Detection Method:

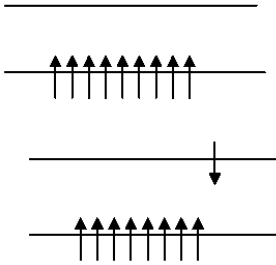

Odd filling of Landau levels

Spin-Flip opens up scattering channels

Similar to giant magneto-resistance

Single Spin Detection Methods:

1. Spin Dependent tunneling from a quantum well
   (change charge state from 1 ⇒ 0)

2. Form singlet bound state versus unbound triplet
   (change charge state from 1 ⇒ 2)

Then detect single charge in an FET or Quantum Point Contact transistor

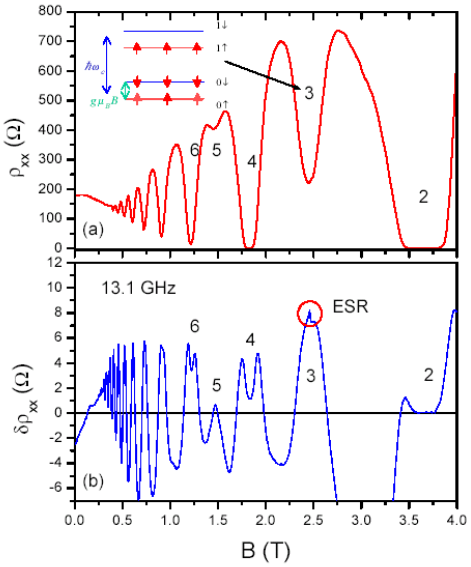

Figure 3. (a) Typical trace of the resistivity ρ_{xx} as a function of the magnetic field. Landau level filling factors ν are indicated. Inset: energy diagram for the case of ν = 3. (b) The microwave radiation induced resistivity change $\delta\rho_{xx}$. Note the ESR feature around ν = 3.

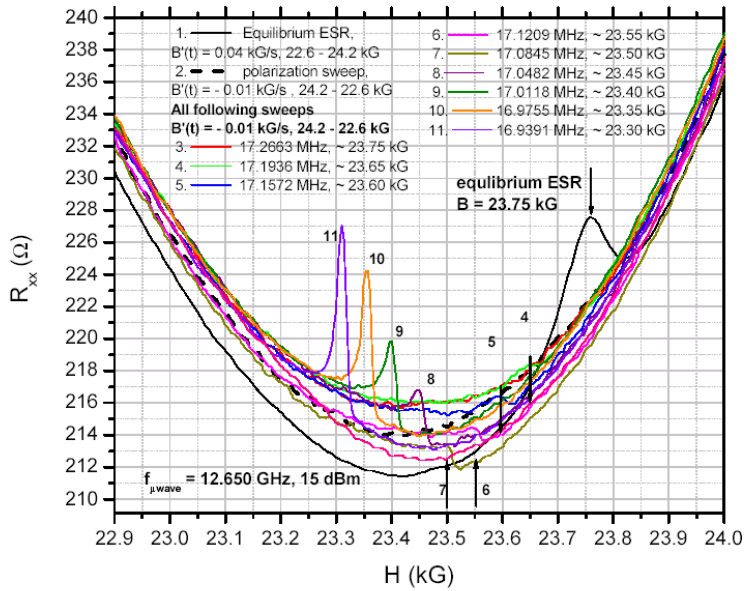

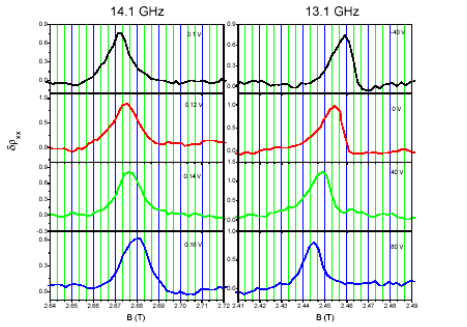

Fig. 4. Electrically detected electron spin resonance spectra at a sequence of gate voltages for (a), a front gate and, (b), a back gate. For the front gate case, the resonant peak moves progressively to higher magnetic field when the amplitude of the bias gate voltage is increased. In contrast, the peak shifts towards lower field for the back gate case. (The non-resonant background of the signal was subtracted for clarity. This task can be easily done since the background varies smoothly over a much broader range of magnetic field.)

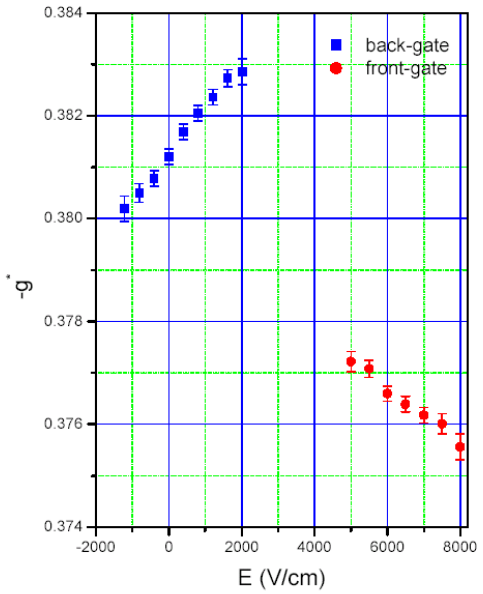

Figure 5. Experimentally determined electronic g-factor as a function of the applied electric field for both the front and back gate. The electric field is simply the applied voltage divided by insulator thickness. In this plot, no attempt was made to include space charge self-consistently.

Spin Detection Method:

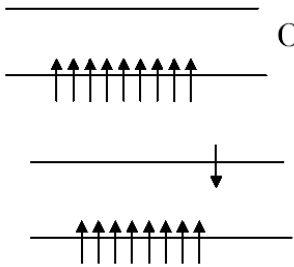

Odd filling of Landau levels

Spin-Flip opens up scattering channels

Similar to giant magneto-resistance

Single Spin Detection Methods:

1. Spin Dependent tunneling from a quantum well
   (change charge state from 1 ⇒ 0)

2. Form singlet bound state versus unbound triplet
   (change charge state from 1 ⇒ 2)

Then detect single charge in an FET or Quantum Point Contact transistor

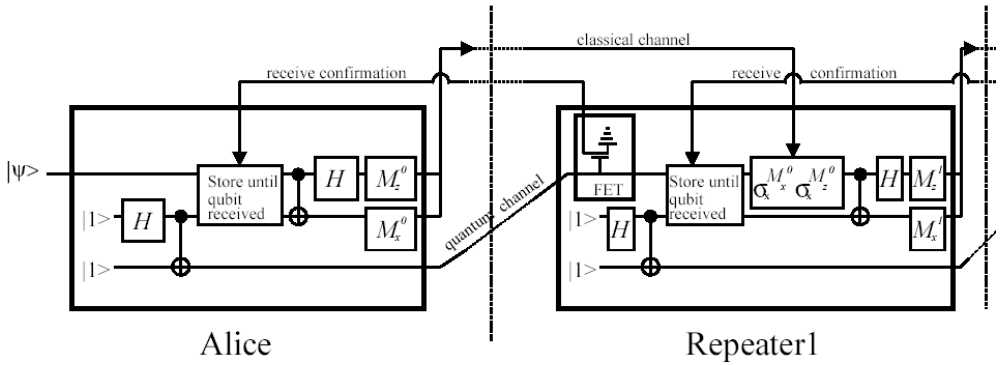

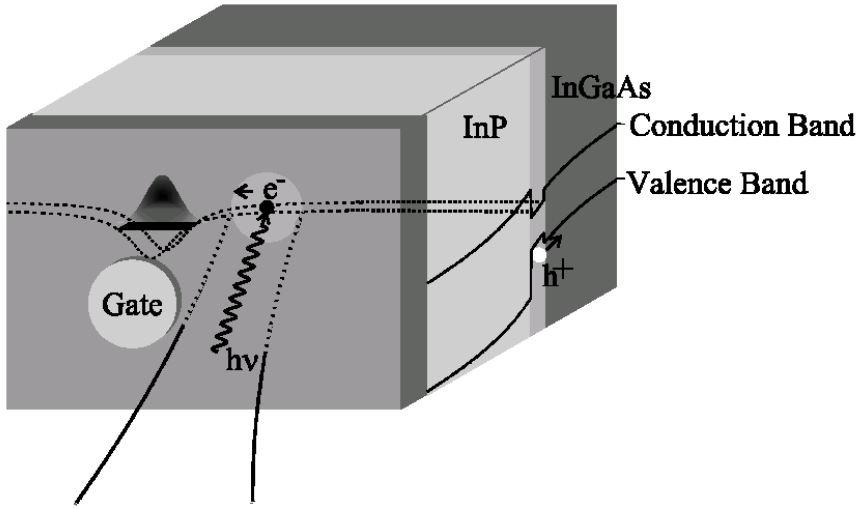

Entanglement Preserving Spin-Coherent Semiconductor Photodetector

Entanglement Preserving Photo-Detector

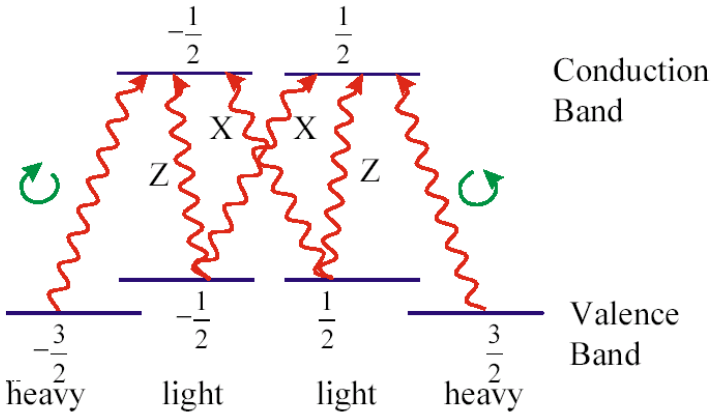

The hole wave functions in Semiconductors:

$|J= 3/2, L=1, S=½\rangle$

heavy $|m_J = 3/2\rangle = |m_l = 1,\ m_s = ½\rangle$

light $|m_J = 1/2\rangle = |m_l = 1, m_s = -½\rangle + |m_l = 0, m_s = ½\rangle$

light $|m_J = -1/2\rangle = |m_l = -1, m_s = ½\rangle - |m_l = 0, m_s = -½\rangle$

heavy $|m_J = -3/2\rangle = |m_l = -1,\ m_s = -½\rangle$

The electron wave function in III-V semiconductors:

$|L=0, S=½\rangle$

electron $|m_l = 0, m_s = ½\rangle$
electron $|m_l = 0, m_s = -½\rangle$

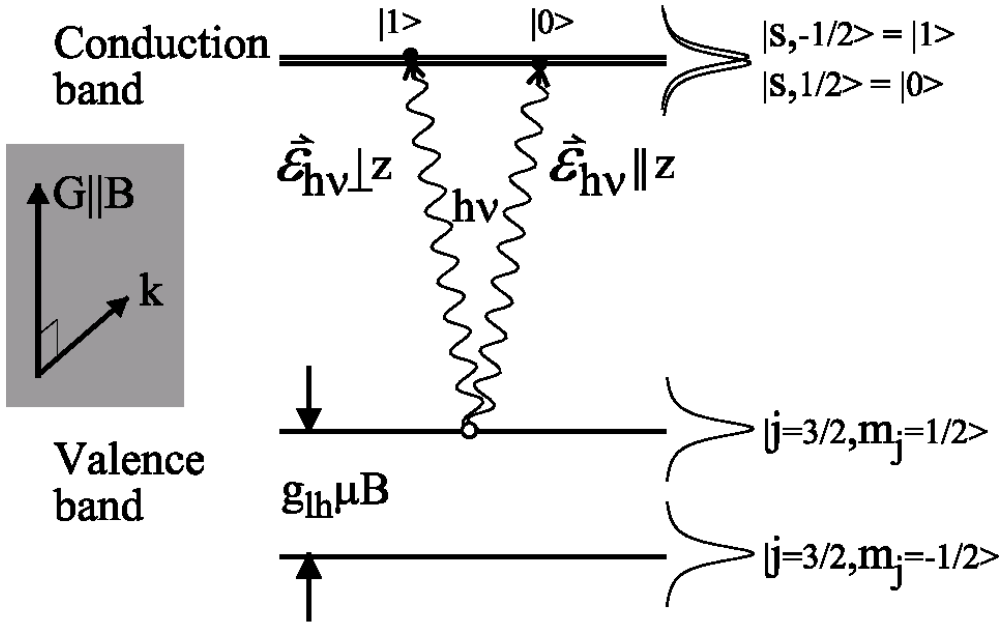

Detecting Entanglement:

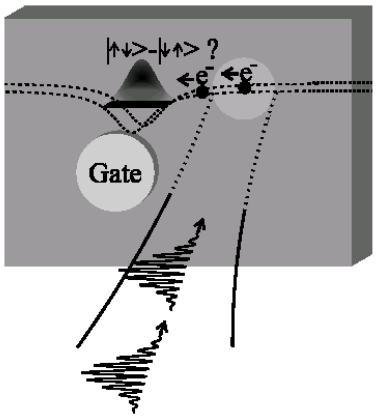

Parametric Decay Photon Pair Generator

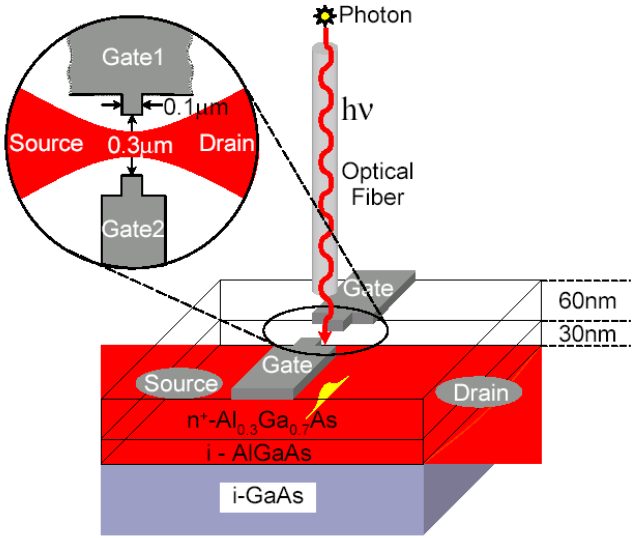

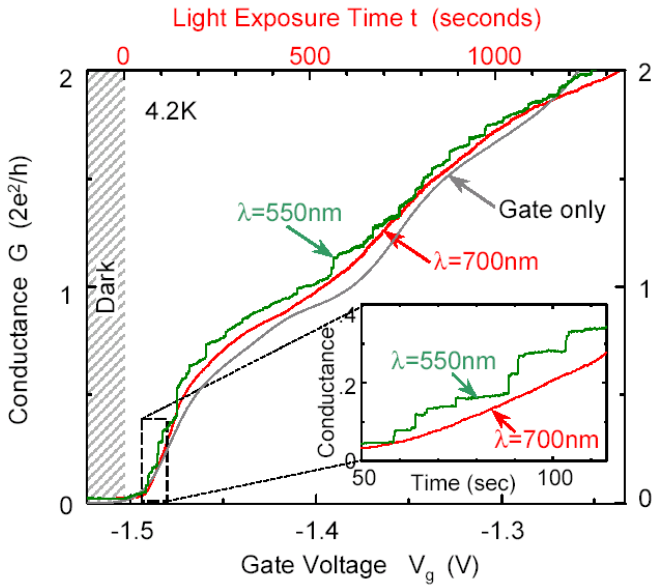

Fig. 1(a) Hideo Kosaka et al.

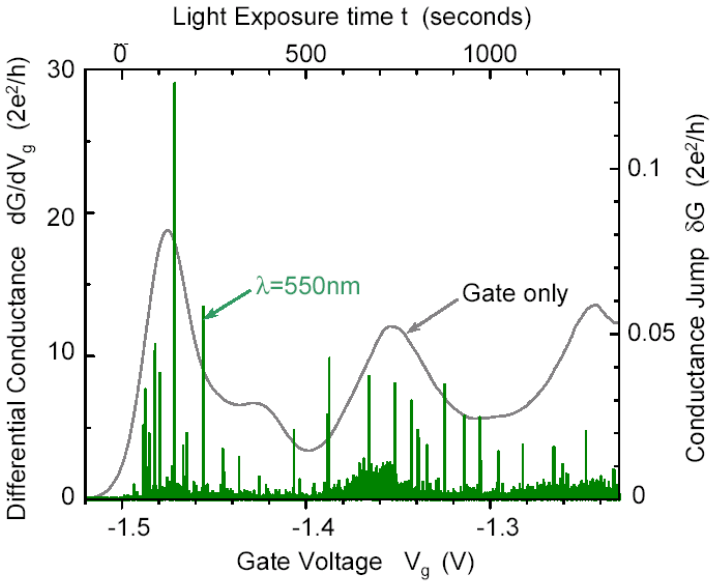

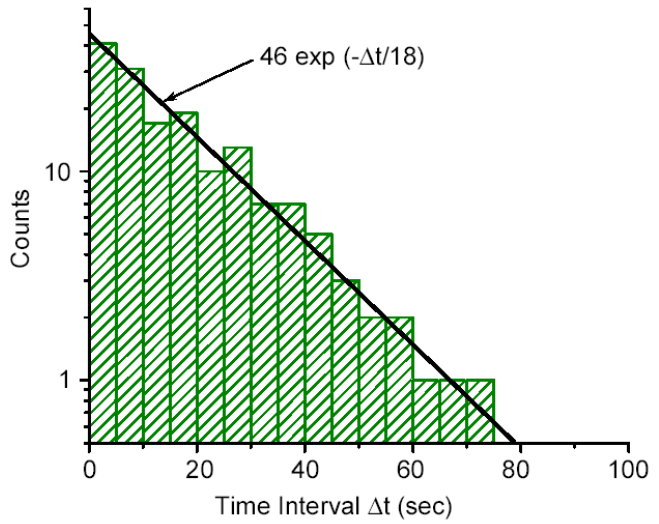

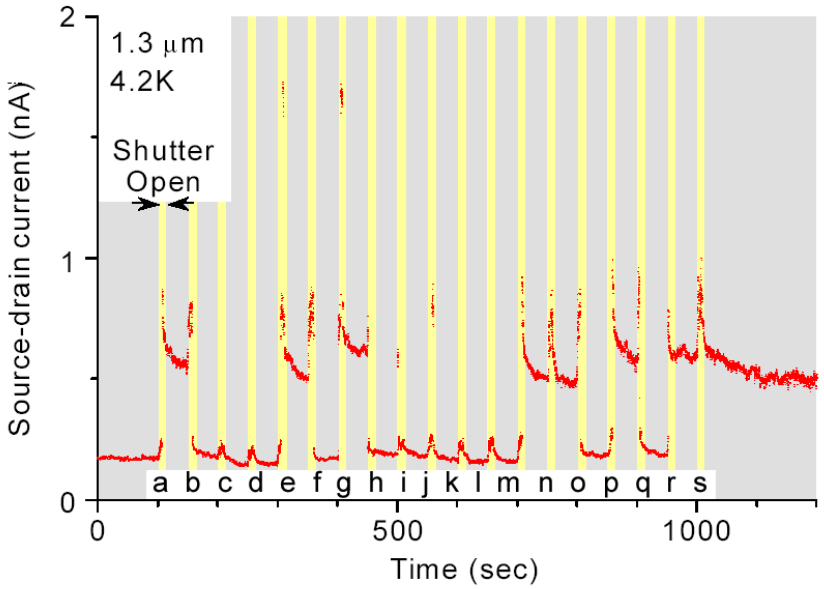

Hideo Kosaka Fig. 5

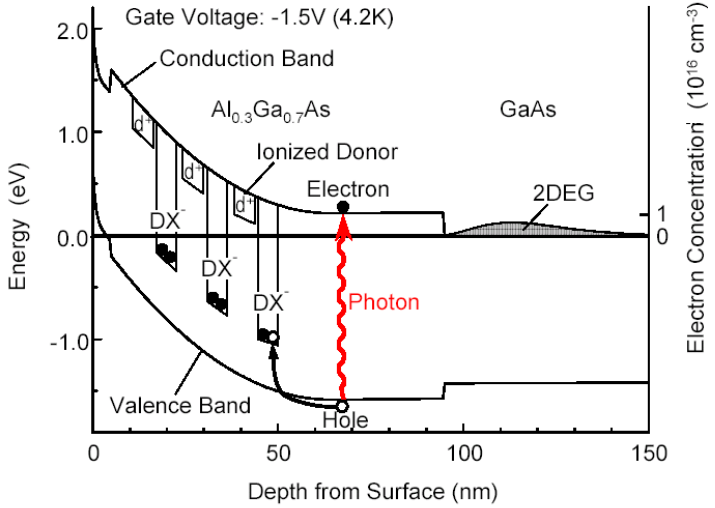

VOLUME 62, NUMBER 21 PHYSICAL REVIEW LETTERS 22 MAY 1989

Direct Observation of the Precession of Individual Paramagnetic Spins on Oxidized Silicon Surfaces

Y. Manassen, R. J. Hamers, J. E. Demuth, and A. J. Castellano, Jr.
IBM Research Division, T. J. Watson Research Center, Yorktown Heights, New York 10598
(Received 12 December 1988)

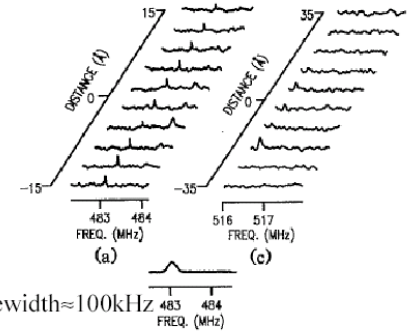

linewidth≈100kHz

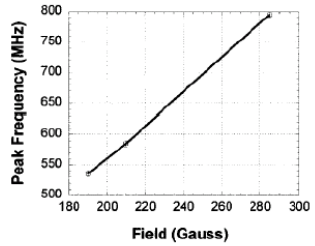

FIG. 5. Plot of the center frequency of STM-ESR peaks on clusters as a function of the applied magnetic field. From this, we obtain a value of $g=2\pm0.1$.

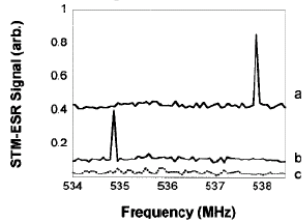

FIG. 3. STM-ESR spectra of (a), (b) two different areas (a few nm apart) of the molecule-covered sample and (c) bare HOPG. The graphs are shifted vertically for clarity.

APPLIED PHYSICS LETTERS VOLUME 80, NUMBER 3 21 JANUARY 2002

Electronic spin detection in molecules using scanning-tunneling-microscopy-assisted electron-spin resonance

C. Durkan[a)] and M. E. Welland
Nanoscale Science Laboratory, Department of Engineering, University of Cambridge, Trumpington Street,

Pentacene in *p*-terphenyl

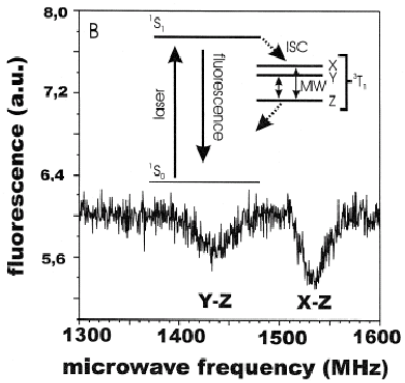

ESR

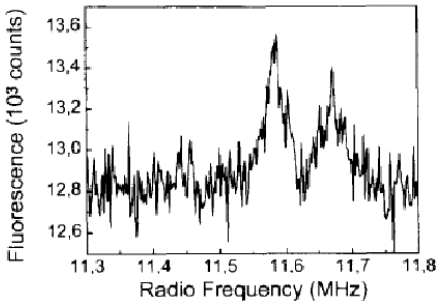

Fig. 3. ENDOR spectrum of a single molecule recorded with a microwave excitation at 1512 MHz, corresponding to the central peak in the ESR spectrum in Fig. 2. 3500 scans with a duration of 0.8 s have been accumulated.

NMR

J. Wrachtrup, A. Gruber, *TU Chemnitz, Inst. of Physics, 09107 Chemnitz, Germany*
SSNMR vol.11, 59–64 (1998)

J. Wrachtrup, A. Gruber, *TU Chemnitz, Inst. of Physics, 09107 Chemnitz, Germany*
Chem. Phys. Lett. 267, 179-185 (1997)

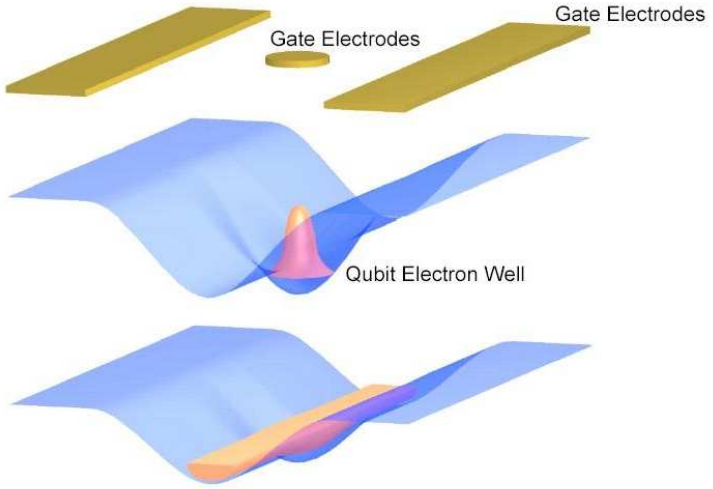

Qubit Read-out Scheme

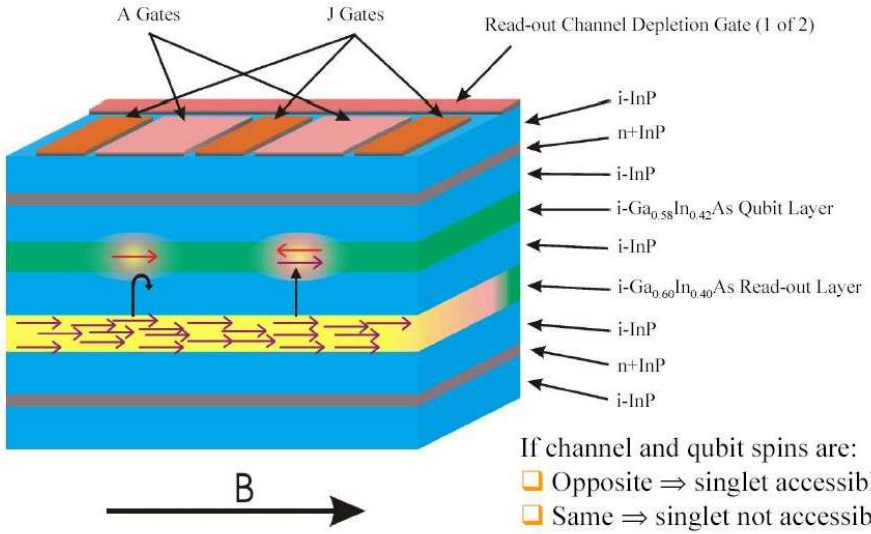

If channel and qubit spins are:

- Opposite ⇒ singlet accessible
- Same ⇒ singlet not accessible

Channel conductivity registers number of electrons in the qubits

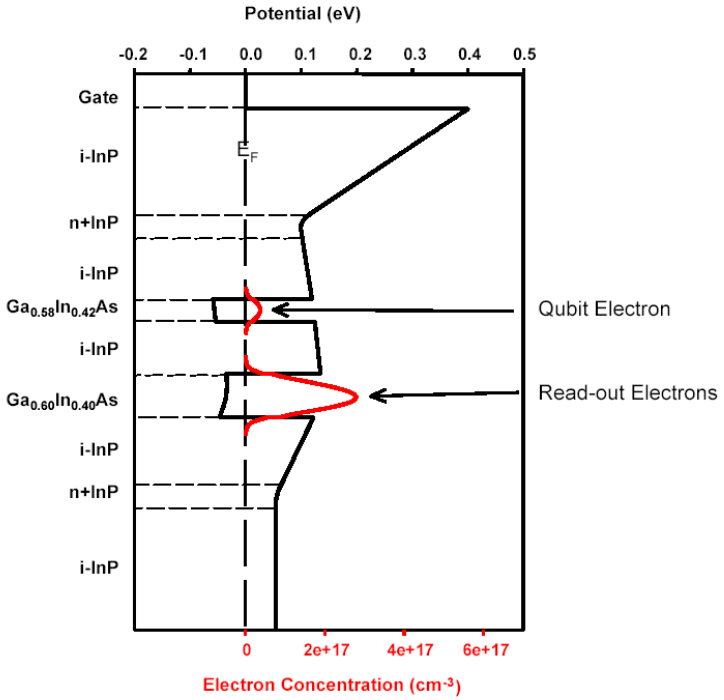

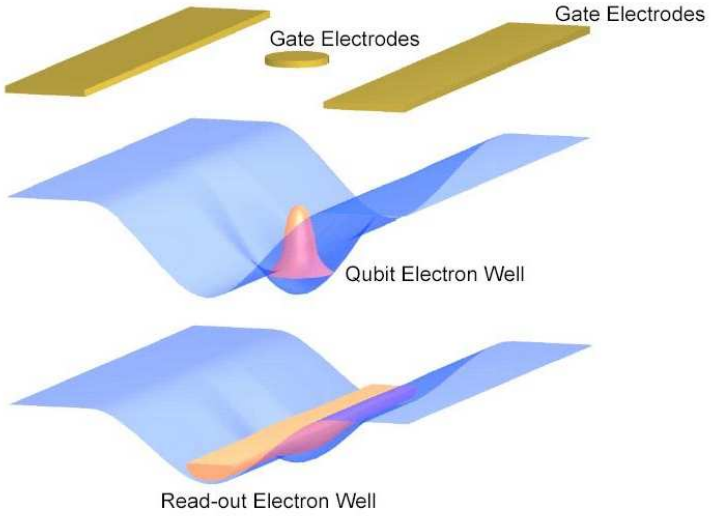

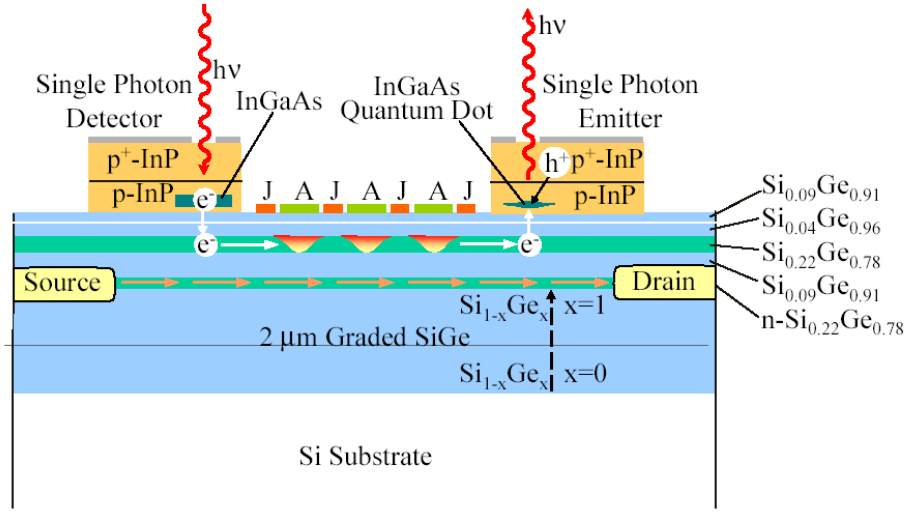

Teleportation Repeater Top-view Schematic

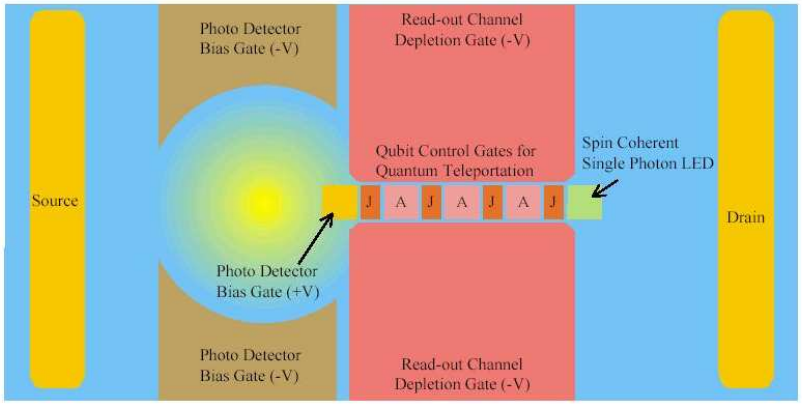

Gates for Quantum Repeater

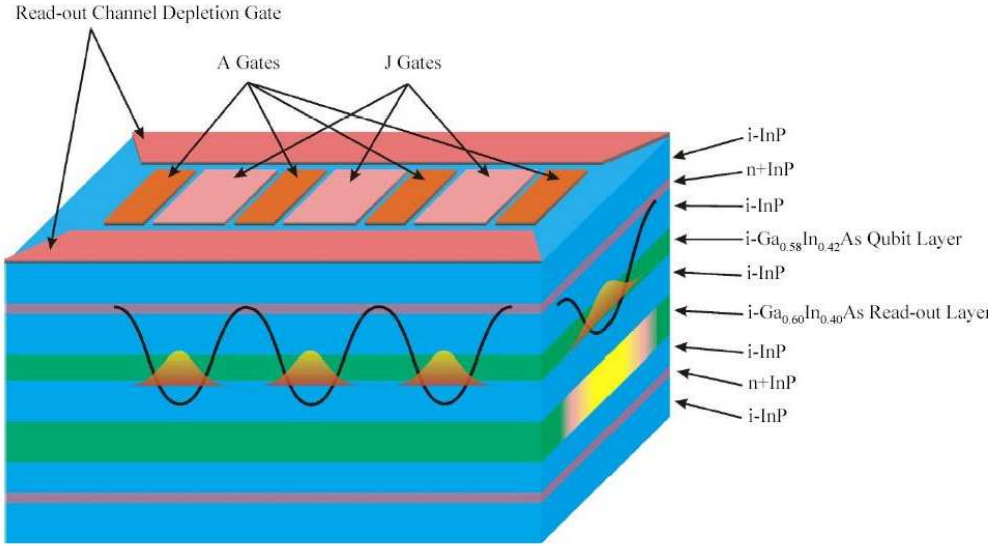

Two qubit interaction

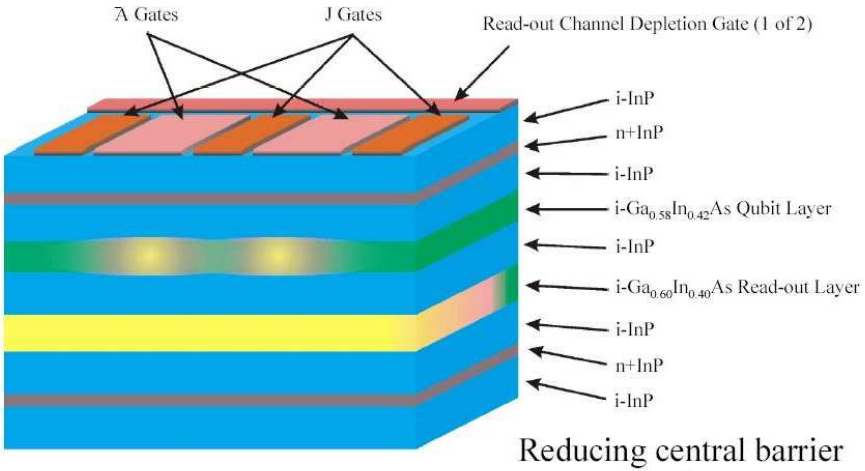

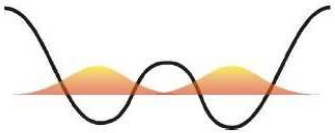

Reducing central barrier turns on exchange interaction between two qubits

Conclusions:

1. There is *little or no penalty* in using electron spins in Silicon versus nuclear spins.

2. Electron spin Dephasing is already slow enough to easily permit error correction.

3. Single photon and single photo-electric charge detection is readily performed in transistor-like structures.

4. The next big step prior to an electron spin CNOT gate is the readout of a single electron spin orientation.

5. In the long run;
Carbon-based electron-spin hosts may allow room temperature operation of a quantum information processor.

Acknowledgements:
•Prof. Karoly Holczer, UCLA Physics Dept.
Spin Echo ESR in Silicon including temperature dependence

•Prof. HongWen Jiang, UCLA Physics Dept.
Gate controlled ESR experiment in a transistor structure

•Dr. Hideo Kosaka, Visiting Scientist, UCLA & NEC Japan & Mr. Deepak Rao, student, UCLA EE Dept.
Single photon detection by Photoconductive Gain experiment

•Dr. Hans Robinson, post-doc, UCLA EE Dept.
Spin readout device design

•Dr. Rutger Vrijen, former post-doc, now at SUN Microsystems Lab
Entanglement preserving photodetector

QUANTUM INFORMATION SPINTRONICS

Electron Spins ..... logic & storage
(in Si)

Nuclear Spins ..... storage
(in Si)

Electron Spins ..... tele-communication
(in III-V)

requires confinement energy >1°K,
thus small quantum dots are not needed;
e-beam lithography is adequate.

Technology Generation	Technology	Gate Count
1	Quantum Key Distribution (fairly Robust) - Heralded –Single-Photon transmitters (Yamamoto et al)	0
2	Quantum Repeater – long distance EPR pair distribution detect photo electron (don't perturb spin)	3
3	Quantum memory – higher secure throughput	≥10
4	Quantum Error Correction	≥40
5	Quantum Factorization Engine	≥1000